Proteomic surfaceome analysis of mesothelioma

Ziegler, A ; Cerciello, F ; Bigosch, C ; Bausch-Fluck, D ; Felley-Bosco, E ; Ossola, R ; Soltermann, A ; Stahel, R A ; Wollscheid, B

Abstract: Identification of new markers for malignant pleural mesothelioma (MPM) is a challenging clinical need. Here, we propose a quantitative proteomics primary screen of the cell surface exposed MPM N-glycoproteins, which provides the basis for the development of new protein-based diagnostic assays. Using the antibody-independent mass-spectrometry based cell surface capturing (CSC) technology, we specifically investigated the N-glycosylated surfaceome of MPM towards the identification of protein-marker candidates discriminatory between MPM and lung adenocarcinoma (ADCA). Relative quantitative CSC analysis of MPM cell line ZL55 in comparison with ADCA cell line Calu-3 revealed a bird's eye view of their respective surfaceomes. In a secondary screen of fifteen MPM and six ADCA, we used high throughput low density microarrays (LDAs) to verify specificity and sensitivity of nineteen N-glycoproteins overregulated in the surfaceome of MPM. This proteo-transcriptomic approach revealed thy-1/CD90 (THY1) and teneurin-2 (ODZ2) as protein-marker candidates for the discrimination of MPM from ADCA. Thy-1/CD90 was further validated by immunohistochemistry on frozen tissue sections of MPM and ADCA samples. Together, we present a combined proteomic and transcriptomic approach enabling the relative quantitative identification and pre-clinical selection of new MPM marker candidates.

DOI: https://doi.org/10.1016/j.lungcan.2011.07.009

Proteomic Surfaceome Analysis of Mesothelioma

Annemarie Ziegler[*,1,†], Ferdinando Cerciello[*,1,3], Colette Bigosch[1,‡], Damaris Bausch-Fluck[3], Emanuela Felley-Bosco[1], Reto Ossola[3], Alex Soltermann[2], Rolf A. Stahel[1], Bernd Wollscheid[3]

[1]Clinic of Oncology, and [2]Institute for Surgical Pathology, University Hospital Zürich, 8044 Zürich, Switzerland

[3]Institute of Molecular Systems Biology, Swiss Federal Institute of Technology (ETH), 8093 Zürich, Switzerland

*AZ and FC contributed equally to this work

[†]Present address: Centro de Genética Humana, Clínica Alemana-Universidad del Desarrollo, Santiago, Chile

[‡]Present address: Umweltmikrobiologie, EAWAG, Dübendorf, Switzerland

Correspondence to

Dr. Bernd Wollscheid
ETH Zürich, Institute of Molecular Systems Biology (IMSB)
HPT D77, Wolfgang-Pauli-Strasse 16
CH-8093 Zürich
Phone: +41 44 633 36 84
Fax: +41 44 633 10 51
E-Mail: bernd.wollscheid@imsb.biol.ethz.ch

Dr. med. Ferdinando Cerciello
ETH Zürich, Institute of Molecular Systems Biology (IMSB)
HPT E52, Wolfgang-Pauli-Strasse 16
CH-8093 Zürich
Phone: +41 44 633 68 56
Fax: +41 44 633 10 51
E-Mail: cerciello@imsb.biol.ethz.ch

Abstract

The identification of new markers for malignant pleural mesothelioma (MPM) is a challenging clinical need. Here, we propose a quantitative proteomics primary screen of the cell surface exposed MPM N-glycoproteins, which provide the basis for the development of new protein-based diagnostic assays. Using the antibody-independent mass-spectrometry based cell surface capturing (CSC) technology, we specifically investigated the N-glycosylated surfaceome of MPM towards the identification of protein-marker candidates discriminatory between MPM and lung adenocarcinoma (ADCA). Relative quantitative CSC analysis of MPM cell line ZL55 in comparison with ADCA cell line Calu-3 revealed a bird's eye view of their respective surfaceomes. In a secondary screen of fifteen MPM and six ADCA, we used high throughput Low Density Microarrays (LDAs) to verify specificity and sensitivity of nineteen N-glycoproteins overregulated in the surfaceome of MPM. This proteo-transcriptomic approach revealed thy-1/CD90 (THY1) and teneurin-2 (ODZ2) as protein-marker candidates for the discrimination of MPM from ADCA. Thy-1/CD90 was further validated by immunohistochemistry on frozen tissue sections of MPM and ADCA samples. Together, we present a combined proteomic and transcriptomic approach enabling the relative quantitative identification and pre-clinical selection of new MPM marker candidates.

Keywords: Mesothelioma, Surfaceome, Cell Surface Capturing (CSC) technology, N-glycoproteins, Surface markers, CD90, ODZ2.

1. Introduction

Malignant pleural mesothelioma (MPM) is an aggressive disease mainly caused by asbestos exposure [1]. The diagnosis requires immunohistochemistry (IHC), combining panels of antibodies against MPM markers (positive for MPM) like calretinin, podoplanin (clone D2-40), cytokeratins 5/6 or WT-1 together with carcinoma-markers (negative for MPM) like epithelial cell adhesion molecule (Ep-CAM, clone Ber-EP4), carcinoembryonic antigen (CEA) or thyroid transcription factor-1 (TTF-1). However, the discrimination of MPM from other malignancies affecting the lung can be difficult. Particularly, the distinction between MPM and lung adenocarcinoma (ADCA) is most challenging [3]. Recently, antibody-independent approaches have evolved as alternative tools for the discrimination of the two diseases, based on gene expression-ratios, RT-PCR or DNA-methylation profiles [4-7]. Despite promising laboratory-based results, the translation of similar techniques into clinical routine remains problematic [8-10].

Here, we propose a combined proteomic and transcriptomic strategy for the identification and selection of new protein-markers for the discrimination between MPM and ADCA. First, we applied the recently developed mass-spectrometry (MS) based cell surface capturing (CSC) technology [11] towards the discovery of the N-glycosylated surfaceome of MPM and ADCA cells. Thereafter, we used the higher throughput Low Density Microarray (LDA) technique, to assess MPM specificity of selected N-glycoproteins on a larger panel of MPM and ADCA cell lines. Our approach revealed thy-1/CD90 (THY1) and teneurin-2 (ODZ2) as new MPM marker candidates. Using a commercially available antibody, we verified thy-1/CD90 expression in tumor samples by IHC, showing that results from our proteo-transcriptomic approach can potentially be directly translated into diagnostic routine.

2. Materials and Methods

2.1. Cell culture

Primary MPM cell cultures were derived from tumor specimens obtained at the time of surgery from patients at the University Hospital Zürich with a confirmed diagnosis, or were derived from MPM malignant pleural-effusions, as previously described [12]. The study was approved by the Ethics Committee of the University Hospital Zürich and written informed consent was obtained from all patients. Primary tumor cultures were characterized by immunodetection of the MPM markers mesothelin, calretinin, wt-1, podoplanin (clone D2-40), N-cadherin and vimentin. MPM cell lines MSTO-211H, H2052, H2452 and H226 were from American Type Culture Collection ATCC (Manassas, VA), ZL55 was established in our laboratory [13]. MPM cells were cultured as described before [12]. The ADCA cell lines Calu-3, A549, Calu-6, SK-LU-1 and the adeno-squamous lung cancer cell line H596 were from ATCC, ZL25 was established in our laboratory [14]. ADCA cells were cultured in RPMI-1640 (Gibco/Invitrogen) with 10% FCS, 2 mM L-glutamine, 1% (w/v) penicillin/streptomycin. All cell lines were maintained at 37°C in a humidified atmosphere with 5% CO_2.

2.2. Cell Surface Capturing (CSC) and mass-spectrometric analysis

SILAC labelling, CSC and mass spectrometric analysis of the MPM cell line ZL55 and the ADCA cell line Calu-3 were performed as previously described [11] [15]. Heavy-Lysine and heavy-Arginine (L-Lysine-$^{13}C_6$,$^{15}N_2$ and L-Arginine-$^{13}C_6$,$^{15}N_4$, Sigma) were used according to the manufacturer's instructions. All MS/MS spectra were converted to mzXML and searched against the UniProt database (Version 57.15)

using the SEQUEST algorithm. Statistical data-analysis was performed using a combination of ISB (Institute of Systems Biology, Seattle) open-source software tools (PeptideProphet™, ProteinProphet™, TPP version 4.3.1; http://tools.proteomecenter.org/software.php). A ProteinProphet protein probability score of at least 0.9 was used for data-filtering, followed by manual validation. Quantitative SILAC data analysis was performed using the XPRESS software [16, 17]. Data was imported, stored, annotated and validated within the in-house developed SISYPHUS database software.

2.3. Low Density Arrays (LDAs)

Cell lines were grown to ~80% confluence in 25 cm^2 flasks, and total RNA was isolated using the RiboPure kit (Ambion, Austin, TX) as indicated by the manufacturer. RNAs were recovered in 50 μl elution buffer and concentrations determined by spectrophotometric measurement in a NanoDrop ND-1000 (Thermo Scientific, Wilmington, DE) device. For synthesis of cDNA, 750 ng total RNA were reverse-transcribed using the High-Capacity cDNA Reverse-Transcription kit (Applied Biosystems, Foster City, CA) in a total volume of 30 μl, following the manufacturer's instructions. This amount had been experimentally determined to warrant synthesis of cDNA and subsequent amplification by real-time PCR under non-saturated, linear conditions. The quality of cDNA was verified by PCR amplification of a β2-microglobulin fragment in 50 μl reactions containing 2 μl cDNA, 1x Buffer II (Applied Biosystems), 1.5 mM $MgCl_2$, 0.13 μM each primer, 0.2 mM each dATP, dTTP, dCTP, and dGTP, and 1.25 units AmpliTaq Gold (Applied Biosystems). Amplification conditions were: 1 cycle at 95ºC for 6 min, 35 cycles at 95ºC for 45 seconds, 60ºC for 1 min, and 72ºC for 30 sec, followed by one final cycle

131 at 72ºC for 10 min. Primer sequences were: β2-F, 5'-
132 GTGGAGCATTCAGACTTGTCTTTCAGC-3', and β2-R, 5'-
133 TTCATCCAATCCAAATGCGGCATCTTC-3´. PCR products were visualized by
134 electrophoresis on polyacrylamide gels. Low Density Arrays for analysis of 22 genes
135 (three internal controls) were obtained from Applied Biosystems. Each LDA slot was
136 loaded with 100 μl solution containing 1x Universal Master Mix (Applied
137 Biosystems) and 10 μl cDNA. PCR amplification was performed in a 7900HT Fast
138 Real-Time PCR System (Applied Biosystems) apparatus using following cycle
139 conditions: 1 cycle of 50ºC for 2 min, 1 cycle of 94ºC for 10 min, and 40 cycles of
140 97ºC for 30 sec, 60ºC for 1 min. Relative gene expression was calculated by using the
141 $2^{-\Delta\Delta Ct}$ method [18]. For each sample, three technical replicates were measured and
142 averaged before performing calculation. 18s and GAPDH were used as internal
143 references.

144 **2.4. Western blot**

145 Detection of mesothelin and N-cadherin was performed on the MPM cell line ZL55
146 and the ADCA cell line Calu-3 by Western blot as previously described [12].
147 Detection of thy-1/CD90 was performed without reducing agents on RIPA-buffer
148 (Upstate Biotech-Millipore, Lake Placid, NY) lysates of the MPM cell lines ZL55 and
149 SDM5, and the ADCA cell lines Calu-3 and SK-LU-1, using a monoclonal anti-thy-1
150 antibody (clone AS02, - Dianova, Hamburg, Germany) at 1:5000 dilution [19]. For
151 sample deglycosylation, cell lysates were incubated overnight with 5 U/mg PNGaseF
152 (Roche, Basel, Switzerland) at 37ºC.

153 **2.5. Immunofluorescent staining.**

Immunofluorescent staining was performed on the ZL55 MPM cells and the Calu-3 ADCA cells after fixation with 4% paraformaldehyde and permeabilization with 0.1% TritonX-100 on uncoated coverslips. Antibody clone 5E10 (BD-Pharmingen, San Diego, CA) was used at 1:100 dilution for thy-1/CD90 detection. Mouse IgG1κ at 1:100 (BD-Pharmingen) was used as specificity isotype-control. Cells were counterstained with Alexa Fluor-488-conjugated cholera-toxin (Invitrogen) at 1:5000 dilution and DAPI (Sigma-Aldrich) at 1:1000 dilution. Images were acquired by confocal laser-scanning microscopy on a TCS-SPE microscope (Leica Microsystems, Wetzlar, Germany) at 63x magnification and processed (brightness and contrast adjustments and necessary cropping) using the Java-based program ImageJ (National Institute of Health, http://rsb.info.nih.gov/ij/).

2.6. Tissue samples and immunohistochemistry

Fresh frozen human tumor specimens were obtained from the Biobank at the Institute for Surgical Pathology, University Hospital Zürich. Corresponding formalin-fixed, paraffin-embedded tumor tissues were processed and diagnoses reported according to the guidelines of the Swiss Society of Pathology. Immunohistochemistry was performed on ice-cold, acetone fixed, frozen whole sections of 5 μm thickness after endogenous peroxidase quenching. Thy-1/CD90 detection was performed using the antibody-clone 5E10 (BD-Pharmingen) at 1:20 dilution and the Vectastain Elite ABC Universal Kit (Vector Laboratories) according to the manufacturer's instructions. Immunoreactivity was visualized by incubation with 3,3'-diaminobenzidine tetrahydrochloride (Vector Laboratories) followed by counterstaining with haematoxylin QS (Vector laboratories). Mouse IgG1κ (BD-Pharmingen) at 1:20 was

used as specificity isotype-control. For each sample, stroma staining-intensity was used as internal reference.

3. Results

3.1. SILAC-based CSC proteomic analysis of N-glycosylated surface proteins

In order to identify differences in-between the surfaceomes of MPM and ADCA we used a SILAC-based CSC proteomic strategy (Fig. 1). The MPM cell line ZL55 and the ADCA cell line Calu-3 were grown in media containing heavy or light isotope forms of the aminoacids arginine and lysine, respectively (SILAC protocol) [20]. The incorporation of different aminoacid isotopes allows to mix the two cell types in equal amounts before lysis and to process them together. MS discrimination between MPM-derived proteins (containing heavy forms of arginine and lysine) and ADCA proteins (containing light forms of arginine and lysine) is then possible based on the mass differences of the incorporated heavy and light peptide isoforms. Following the CSC protocol, the sugar moieties of the cell surface exposed glycoproteins are labelled with biotin hydrazide on the living cells and, after protein digestion with trypsin, the glycopeptides are enriched with streptavidin coated beads. Using the enzyme PNGaseF, N-glycosylated peptides are then specifically released and analyzed via microfluidic LC-MS/MS. Overall, 100 cell surface N-glycoproteins, including 37 CD annotated proteins, were identified (Supplementary Table ST1). The MS analysis also revealed 211 MPM/ADCA N-glycopeptides containing a deamidation signature within the NXS/T motif, indicating the specific isolation and PNGaseF-mediated release of those N-glycopeptides via CSC (Supplementary Table ST2). We thereafter used the software XPRESS to calculate abundance ratios between the MPM and ADCA proteins. Among the glycoproteins upregulated in MPM, we identified the

known MPM markers mesothelin (UniProt ID MSLN_human, Q13421; Entrez gene name MSLN) and N-cadherin (synonyms CD325, Cadherin-2; UniProt ID CADH2_human, P19022; Entrez gene name CDH2) (Fig. 2A) The clear upregulation of the two proteins detected by MS in ZL55 (mesothelin abundance-ratio calculated with the software XPRESS revealed a ratio of ADCA over MPM of 0.04 ± 0.00 and for N-cadherin an abundance-ratio of 0.05 ± 0.04) matched the results obtained by Western blot (WB) (Fig. 2B), confirming the specificity of our approach.

3.2. Semi-quantitative RT-PCR cell lines screening for MPM cell surface glycoprotein-marker candidates

In the next set of experiments, we used LDAs in order to further qualify the initial MPM glycoprotein markers at the transcription level on a larger panel of representative and diverse MPM and ADCA cell lines (Table 1). The mRNA expression of 19 pre-qualified N-glycoproteins from the proteomic screen, including mesothelin and N-cadherin as landmark proteins, was analyzed in fifteen MPM and six ADCA cell lines (Fig. 3 and supplementary table ST3). Mesothelin transcript was expressed in ten out of fifteen (67%) MPM cell lines and in the adeno-squamous cell line H596. N-cadherin was expressed in all (100%) MPM and also in three (50%) ADCA cell lines. Among the other investigated genes, thy-1/CD90 (synonym CD90; UniProt ID THY1_human, P04216; Entrez gene name THY1) and teneurin-2 (UniProt ID TEN2_human, Q9NT68; Entrez gene name ODZ2) displayed a selective association with MPM (Fig. 3A and B). Thy-1/CD90 (THY1) showed homogenous mRNA expression in MPM and was absent from ADCA cell lines. Teneurin-2 (ODZ2) was expressed in eleven MPM cell lines, but only at low levels in one ADCA (SK-LU-1) and one adeno-squamous cell line (H596). All other candidates presented

225 a heterogeneous expression profile without individual discriminatory power between
226 MPM and ADCA.

227 **3.3. Western blot verification of thy-1 in MPM and ADCA cell lines**

228 As a first step to verify our markers by immunologic assays, we tried to acquire
229 suitable antibodies. Since no antibody for human teneurin-2 was commercially
230 available, we generated a rabbit anti-serum against two extracellular peptides
231 identified in the proteomic screens from teneurin-2. However, no specific signals
232 could be detected in WB and IHC experiments (data not shown). For thy-1/CD90, we
233 tested a series of commercially available antibodies (data not shown) and selected the
234 mouse clone AS02 to compare thy-1/CD90 expression in two MPM (ZL55, SDM5)
235 and two ADCA (Calu-3, SK-LU-1) cell lines by WB (Fig. 4). Chemoluminescent
236 signals of the appropriate molecular weight were obtained for deglycosylated thy-
237 1/CD90 in MPM cells (lane 6 and 8), but not in ADCA cells (lane 2 and 4). Only in
238 the MPM SDM5 cell line, thy-1/CD90 protein was also recognized in its
239 glycosylated, higher molecular weight form (lane 7).

240 **3.4. Immunohistochemical verification of thy-1 in human tissues**

241 We further set out to validate our proteo-transcriptomic approach in IHC assays. In
242 our hands, the anti-thy-1 clone AS02 did not perform satisfactory on tissues (data not
243 shown), thus, we tested additional commercially available antibodies and selected the
244 clone 5E10. It has to be mentioned that none of the tested antibodies did perform on
245 formalin-fixed paraffin-embedded (FFPE) tissues (data not shown). In agreement with
246 MS, RT-PCR and WB results, using clone 5E10, thy-1/CD90 expression was detected
247 in MPM, but not in ADCA cell lines (Fig. 5A). The overlay of a cholera-toxin

staining for the plasma membrane associated ganglioside GM1 with anti-thy-1 staining suggests a co-localisation of both molecules at the cell surface. We further used clone 5E10 to investigate human frozen sections from four epithelioid and two biphasic MPM tumors as well as eight ADCA with different grading levels (Fig. 5B, supplementary table ST4). Reaction to anti-thy-1 antibody was observed in the tumor-stromal cells of both tumor types. Three MPM cases presented discrete numbers of tumor cells with moderate membrane staining whereas ADCA cells reacted only modestly, if at all, to anti-thy-1 with weak to moderate cytoplasmic staining of tumors cells toward the stroma.

4. Discussion

In our work we investigated a new approach to the analysis of the MPM surfaceome toward the identification of markers for the discrimination of MPM from ADCA. To do so, we analyzed the surfaceomes of two MPM and ADCA cell lines via the CSC technology. The CSC technology enables the parallel identification of surface exposed N-glycosylated proteins using antibody-independent mass spectrometric techniques. The CSC technology thus allows for large screens of proteins without biases related to antibody availability or quality. To sort for N-glycoproteins associated with MPM, we combined the CSC with the SILAC strategy for relative protein quantitation and selected those proteins showing upregulation in MPM compared to ADCA. The validity of this approach was corroborated by the unbiased detection of the glycoproteins mesothelin and N-cadherin among the proteins with higher abundance in MPM. Both proteins are in fact known to be associated with MPM, even if their specificity is unsatisfactory for clinical application [21-23]. In addition, MS observed overregulation of the two proteins in MPM could be

reproduced and confirmed by antibody-assays (WB). However, it should be mentioned that we could not observe the widely accepted MPM markers calretinin, podoplanin, cytokeratins 5/6 or WT-1. This was due to the fact that these protein-markers are neither cell surface exposed (with the exception of podoplanin) nor N-glycosylated, and thus not accessible by our approach.

Among the N-glycoproteins upregulated in MPM, we focused on those proteins, which were only rarely or not at all reported in the literature in association with MPM before. In order to anticipate the MPM specificity and sensitivity of these selected proteins, we screened fifteen MPM and six ADCA cell lines by LDAs assays. We decided to apply LDAs, owing to the fact that RT-PCR protocols are nowadays standardized, quick, easily accessible and relatively cheap compared to current proteomic approaches. In contrast to screens based solely on mRNA investigations, here we could take advantage of our previous MS analysis, selecting only for genes known to be translated in proteins. Again, to confirm the validity of the approach, we first looked at our landmarks proteins mesothelin and N-cadherin. As expected, none of the two proteins resulted to be a reliable single discriminator for MPM [21-23]. Among the other investigated genes, thy-1/CD90 (THY1) and teneurin-2 (ODZ2) showed the strongest association with MPM. Teneurin-2 (ODZ2) is one of the four members of the teneurin family of proteins. These more than 300 kDa large transmembrane proteins are probably involved in cell-signalling and transcription regulation, but their function is yet unknown [24]. Only few studies report about teneurin-2 in cancer and there is some uncertainty about its potential tumor-suppressor or oncogenic function [25, 26]. Since no commercial antibodies against human teneurin-2 were available, we produced rabbit-antisera against two extracellular peptide sequences. However, reaction of the antibody was

297 unsatisfactory. Thy-1/ CD90 (THY1) is a small, heavily glycosylated GPI-anchored
298 cell surface protein with the highest expression in human among (primarily fetal)
299 thymic stromal cells and most fibroblasts [27]. A tumor-suppressor function of thy-
300 1/CD90 has been proposed in ovarian and nasopharyngeal cancer [28-32], but protein
301 expression in cancer stem-cells has rather been associated with more aggressive
302 behaviour and chemoresistance [33-35]. Recently, thy-1/CD90 has been observed in
303 four MPM cell cultures grown in low serum conditions and a correlation to highly-
304 proliferative or stem-cell-like cells was speculated by the authors [36].

305 We used WB to validate MPM specificity of thy-1/CD90 at protein level.
306 Interestingly, in one MPM case (cell line ZL55), thy-1/CD90 was detectable only
307 after deglycosylation with PNGaseF, pointing out a clear pitfall of approaches based
308 solely on antibodies. Finally, we verified thy-1/CD90 expression in MPM and ADCA
309 tissues by IHC on frozen sections. Three MPM patients presented discrete numbers of
310 tumor cells reacting positively to anti-thy-1 antibody (clone 5E10), while ADCA
311 tumor cells reacted rather weakly and unspecific to the antibody. However, both
312 tumors showed positive reaction of the tumor-stromal cells. To further verify and
313 confirm these preliminary observations in larger scale, suitable antibodies for
314 paraffin-embedded tissues would be essential.

315 **5. Conclusions**

316 Our work investigated a novel proteo-transcriptomic strategy for the identification of
317 MPM biomarkers discriminatory from ADCA. Cell surface analysis with the CSC
318 technology in combination with LDAs enabled the high-throughput and multiplexed
319 screen required for the investigation and pre-clinical selection of new biomarkers.
320 This strategy resulted to be a valid complement to approaches based solely on

antibodies, whose limitations are often related to epitope and application-based constraints. Our results provide evidence that teneurin-2, and especially thy-1/CD90, are cell surface accessible marker candidates for the differentiation of MPM from ADCA.

Acknowledgements

This work was supported by the Cancer League of Zürich and the NCCR Neural Plasticity and Repair of the Swiss National Science Foundation (SNF). F.C. is recipient of a fellowship under the MD-PhD programme of the SNF and student at the MD-PhD and Cancer Biology programs of the University of Zürich. We thank Thomas Bock, Andreas Frei and Hansjörg Möst for fruitful discussion and Dr. Marianne Tinguely and Dr. Andreas Hofmann for critical reading of a draft manuscript.

Conflict of interest statement

Authors declare no conflicting financial interests.

References

1. Berry G, Newhouse ML, Wagner JC. Mortality from all cancers of asbestos factory workers in east London 1933-80. Occup Environ Med 2000; 57: 782-785.
2. Husain AN, Colby TV, Ordonez NG, Krausz T, Borczuk A, Cagle PT, Chirieac LR, Churg A, Galateau-Salle F, Gibbs AR, Gown AM, Hammar SP, Litzky LA, Roggli VL, Travis WD, Wick MR. Guidelines for pathologic diagnosis of malignant mesothelioma: a consensus statement from the International Mesothelioma Interest Group. Arch Pathol Lab Med 2009; 133: 1317-1331.
3. Roberts F, McCall AE, Burnett RA. Malignant mesothelioma: a comparison of biopsy and postmortem material by light microscopy and immunohistochemistry. J Clin Pathol 2001; 54: 766-770.
4. Gordon GJ, Jensen RV, Hsiao LL, Gullans SR, Blumenstock JE, Ramaswamy S, Richards WG, Sugarbaker DJ, Bueno R. Translation of microarray data into clinically relevant cancer diagnostic tests using gene expression ratios in lung cancer and mesothelioma. Cancer Res 2002; 62: 4963-4967.
5. Holloway AJ, Diyagama DS, Opeskin K, Creaney J, Robinson BW, Lake RA, Bowtell DD. A molecular diagnostic test for distinguishing lung adenocarcinoma from malignant mesothelioma using cells collected from pleural effusions. Clin Cancer Res 2006; 12: 5129-5135.
6. Christensen BC, Marsit CJ, Houseman EA, Godleski JJ, Longacker JL, Zheng S, Yeh RF, Wrensch MR, Wiemels JL, Karagas MR, Bueno R, Sugarbaker DJ, Nelson HH, Wiencke JK, Kelsey KT. Differentiation of lung adenocarcinoma, pleural mesothelioma, and nonmalignant pulmonary tissues using DNA methylation profiles. Cancer Res 2009; 69: 6315-6321.
7. Gordon GJ. Transcriptional profiling of mesothelioma using microarrays. Lung Cancer 2005; 49 Suppl 1: S99-S103.
8. Michiels S, Koscielny S, Hill C. Prediction of cancer outcome with microarrays: a multiple random validation strategy. Lancet 2005; 365: 488-492.
9. Draghici S, Khatri P, Eklund AC, Szallasi Z. Reliability and reproducibility issues in DNA microarray measurements. Trends Genet 2006; 22: 101-109.
10. Pollack JR. A perspective on DNA microarrays in pathology research and practice. Am J Pathol 2007; 171: 375-385.
11. Wollscheid B, Bausch-Fluck D, Henderson C, O'Brien R, Bibel M, Schiess R, Aebersold R, Watts JD. Mass-spectrometric identification and relative quantification of N-linked cell surface glycoproteins. Nat Biotechnol 2009; 27: 378-386.
12. Thurneysen C, Opitz I, Kurtz S, Weder W, Stahel RA, Felley-Bosco E. Functional inactivation of NF2/merlin in human mesothelioma. Lung Cancer 2009; 64: 140-147.
13. Schmitter D, Lauber B, Fagg B, Stahel RA. Hematopoietic growth factors secreted by seven human pleural mesothelioma cell lines: interleukin-6 production as a common feature. Int J Cancer 1992; 51: 296-301.
14. Stahel RA, O'Hara CJ, Waibel R, Martin A. Monoclonal antibodies against mesothelial membrane antigen discriminate between malignant mesothelioma and lung adenocarcinoma. Int J Cancer 1988; 41: 218-223.

15. Harsha HC, Molina H, Pandey A. Quantitative proteomics using stable isotope labeling with amino acids in cell culture. Nat Protoc 2008; 3: 505-516.
16. Han DK, Eng J, Zhou H, Aebersold R. Quantitative profiling of differentiation-induced microsomal proteins using isotope-coded affinity tags and mass spectrometry. Nat Biotechnol 2001; 19: 946-951.
17. Li XJ, Zhang H, Ranish JA, Aebersold R. Automated statistical analysis of protein abundance ratios from data generated by stable-isotope dilution and tandem mass spectrometry. Anal Chem 2003; 75: 6648-6657.
18. Livak KJ, Schmittgen TD. Analysis of relative gene expression data using real-time quantitative PCR and the 2(-Delta Delta C(T)) Method. Methods 2001; 25: 402-408.
19. Saalbach A, Aneregg U, Bruns M, Schnabel E, Herrmann K, Haustein UF. Novel fibroblast-specific monoclonal antibodies: properties and specificities. J Invest Dermatol 1996; 106: 1314-1319.
20. Ong SE, Blagoev B, Kratchmarova I, Kristensen DB, Steen H, Pandey A, Mann M. Stable isotope labeling by amino acids in cell culture, SILAC, as a simple and accurate approach to expression proteomics. Mol Cell Proteomics 2002; 1: 376-386.
21. Ordonez NG. Application of mesothelin immunostaining in tumor diagnosis. Am J Surg Pathol 2003; 27: 1418-1428.
22. Ordonez NG. Value of E-cadherin and N-cadherin immunostaining in the diagnosis of mesothelioma. Hum Pathol 2003; 34: 749-755.
23. Ordonez NG. The immunohistochemical diagnosis of mesothelioma: a comparative study of epithelioid mesothelioma and lung adenocarcinoma. Am J Surg Pathol 2003; 27: 1031-1051.
24. Bagutti C, Forro G, Ferralli J, Rubin B, Chiquet-Ehrismann R. The intracellular domain of teneurin-2 has a nuclear function and represses zic-1-mediated transcription. J Cell Sci 2003; 116: 2957-2966.
25. Nathanson KL, Shugart YY, Omaruddin R, Szabo C, Goldgar D, Rebbeck TR, Weber BL. CGH-targeted linkage analysis reveals a possible BRCA1 modifier locus on chromosome 5q. Hum Mol Genet 2002; 11: 1327-1332.
26. Vinatzer U, Gollinger M, Mullauer L, Raderer M, Chott A, Streubel B. Mucosa-associated lymphoid tissue lymphoma: novel translocations including rearrangements of ODZ2, JMJD2C, and CNN3. Clin Cancer Res 2008; 14: 6426-6431.
27. Bradley JE, Ramirez G, Hagood JS. Roles and regulation of Thy-1, a context-dependent modulator of cell phenotype. Biofactors 2009; 35: 258-265.
28. Cao Q, Abeysinghe H, Chow O, Xu J, Kaung H, Fong C, Keng P, Insel RA, Lee WM, Barrett JC, Wang N. Suppression of tumorigenicity in human ovarian carcinoma cell line SKOV-3 by microcell-mediated transfer of chromosome 11. Cancer Genet Cytogenet 2001; 129: 131-137.
29. Abeysinghe HR, Cao Q, Xu J, Pollock S, Veyberman Y, Guckert NL, Keng P, Wang N. THY1 expression is associated with tumor suppression of human ovarian cancer. Cancer Genet Cytogenet 2003; 143: 125-132.
30. Abeysinghe HR, Pollock SJ, Guckert NL, Veyberman Y, Keng P, Halterman M, Federoff HJ, Rosenblatt JP, Wang N. The role of the THY1 gene in human ovarian cancer suppression based on transfection studies. Cancer Genet Cytogenet 2004; 149: 1-10.

31. Lung HL, Cheng Y, Kumaran MK, Liu ET, Murakami Y, Chan CY, Yau WL, Ko JM, Stanbridge EJ, Lung ML. Fine mapping of the 11q22-23 tumor suppressive region and involvement of TSLC1 in nasopharyngeal carcinoma. Int J Cancer 2004; 112: 628-635.
32. Lung HL, Bangarusamy DK, Xie D, Cheung AK, Cheng Y, Kumaran MK, Miller L, Liu ET, Guan XY, Sham JS, Fang Y, Li L, Wang N, Protopopov AI, Zabarovsky ER, Tsao SW, Stanbridge EJ, Lung ML. THY1 is a candidate tumour suppressor gene with decreased expression in metastatic nasopharyngeal carcinoma. Oncogene 2005; 24: 6525-6532.
33. Yang ZF, Ho DW, Ng MN, Lau CK, Yu WC, Ngai P, Chu PW, Lam CT, Poon RT, Fan ST. Significance of CD90+ cancer stem cells in human liver cancer. Cancer Cell 2008; 13: 153-166.
34. Liu G, Yuan X, Zeng Z, Tunici P, Ng H, Abdulkadir IR, Lu L, Irvin D, Black KL, Yu JS. Analysis of gene expression and chemoresistance of CD133+ cancer stem cells in glioblastoma. Mol Cancer 2006; 5: 67.
35. Gupta PB, Onder TT, Jiang G, Tao K, Kuperwasser C, Weinberg RA, Lander ES. Identification of selective inhibitors of cancer stem cells by high-throughput screening. Cell 2009; 138: 645-659.
36. Melotti A, Daga A, Marubbi D, Zunino A, Mutti L, Corte G. In vitro and in vivo characterization of highly purified human mesothelioma derived cells. BMC Cancer; 10: 54.

Legends for figures

Figure 1. *Workflow for the identification and verification of MPM discriminatory marker candidates.* Cell surface capturing (CSC) was applied in combination with SILAC for quantitative analysis of the N-glycosylated cell surface proteins of the MPM cell line ZL55 and the ADCA cell line Calu-3. Differentially regulated proteins were investigated by LDA assays on a panel of MPM and ADCA cell lines. Proteins showing potential specificity for MPM were verified at cell and tissue level by antibody-based assays.

Figure 2. *Detection and quantitation of the reference mesothelioma markers mesothelin and N-cadherin.* **A**, Mass spectrometric quantitation of the mesothelin peptide LAFQNMNGSEYFVK and N-cadherin peptide VDIIVANLTVTDK identified by CSC in the SILAC-heavy-labelled MPM cell line ZL55 and the light-labelled ADCA cell line Calu-3. The XPRESS software was used to define the elution areas of the peptides and calculate the isotopic ratios between light and heavy peptide forms. Elution areas used for quantitation are delimited by the dotted blue curves between the dashed black-lines. The red traces are the peptide chromatograms identified in the elution areas used for quantitation. **B**, Western blot detection of mesothelin and N-cadherin. Reaction against the anti-mesothelin antibody can be detected for the MPM cell line ZL55, but is only weak or absent for the ADCA cell line Calu-3. Similar can be observed using the anti-N-cadherin antibody.

Figure 3. *Mass spectrometric quantitation of the proteins thy-1/CD90 and teneurin-2 and relative mRNA expression as assessed by low density array RT-PCR profiling.* **A**, Elution profiles of the thy-1/CD90 peptide SPPISSQNVTVLR and the teneurin-2

peptide NSSIDSGEAEVGR identified by CSC of the heavy-labeled MPM cell line ZL55 and the light-labeled ADCA cell line Calu-3. Quantitation was calculated with the software XPRESS and derived from the isotopic ratios of the elution areas of the peptides. Dotted blue curves between the dashed black-lines mark elution areas used for relative quantiation. The red traces correspond to the peptide chromatograms identified in the elution areas used for quantitation. B, Graphs show the relative mRNA levels of mesothelin (gene name MSLN), N-cadherin (gene name CDH2), thy-1/CD90 (gene name THY1) and teneurin-2 (gene name ODZ2) in fifteen MPM (dashed bars, cell lines ZL55 to SDM61) and six ADCA (black bars, cell lines Calu-3 to SK-LU-1) cell lines.

Figure 4. *Expression of thy-1/CD90 protein in MPM and ADCA cell lines.* Protein lysates from ADCA cell lines Calu-3 and SK-LU-1 and from MPM cell lines ZL55 and SDM5 were separated on SDS-PAGE (4-12%). For deglycosylation, cell lysates were treated with PNGaseF. Using mouse anti-thy-1 antibody, a band compatible with the size of thy-1/CD90 (28 kDa) was detected in the untreated SDM5 lysates. Upon PNGaseF treatement, signals at 17 kDa were detected in both MPM cell lines, which agree with the weight of deglycosylated thy-1/CD90. Independent of PNGaseF treatement, no signal could be detected for the ADCA cell lines. The position of weight standards is indicated at the left, while - *and* + indicate lysates without and with PNGaseF treatement, respectively.

Figure 5. *Immunofluorescent and immunohistochemical detection of thy-1/CD90.*
A, Immunofluorescent staining of thy-1/CD90 protein in MPM and ADCA cell lines. The MPM cell line ZL55 and the ADCA cell line Calu-3 were stained with mouse anti-thy-1 antibody 5E10 (red). Cell membranes were counterstained with Alexa

Fluor 488-conjugated cholera-toxin (green), and nuclei with DAPI (blue). Merged images are shown at the far right. **B**, Two representative IHC examples of human MPM (*a-b*) and ADCA (*c-d*). Images were recorded at *10x* and representative regions (insets) at *20x* magnification. Reference slides from the same tumors were also stained with haematoxylin-eosin.

550 **Table 1: Cell lines used for LDAs assays**

Cell line	Type	Histology	Origin	Patient (sex/age)	Source/Reference
ZL55	MPM	Epithelioid	Tumor	M/52	Our lab, *ref.13*
SDM5	MPM	Epithelioid	Effusion	M/54	Our lab
SDM13	MPM	Epithelioid	Tumor	M/58	Our lab
SDM16	MPM	Epithelioid	Tumor	M/65	Our lab
SDM22	MPM	Epithelioid	Effusion	M/62	Our lab
SDM46	MPM	Epithelioid	Tumor	M/57	Our lab
SDM47	MPM	Epithelioid	Tumor	M/58	Our lab
SDM48	MPM	Epithelioid	Tumor	M/55	Our lab
SDM55	MPM	Epithelioid	Tumor	M/40	Our lab
SDM57	MPM	Epithelioid	Tumor	F/62	Our lab
SDM61	MPM	Epithelioid	Tumor	M/66	Our lab
MSTO-211H	MPM	Biphasic	Effusion	M/62	Our lab
H2052	MPM	Sarcomatoid	Effusion	M/65	ATCC
H2452	MPM	Epithelioid	Tumor	M/-	ATCC
H226	MPM	Epithelioid	Effusion	M/-	ATCC
Calu-3	NSCLC	ADCA	Effusion	M/25	ATCC
Calu-6	NSCLC	ADCA	-	F/61	ATCC
A549	NSCLC	ADCA	-	M/58	ATCC
SK-LU-1	NSCLC	ADCA	-	F/60	ATCC
ZL25	NSCLC	ADCA	-	M/60	Our lab, *ref.14*
H596	NSCLC	Adenosquamous	-	M/73	ATCC

551

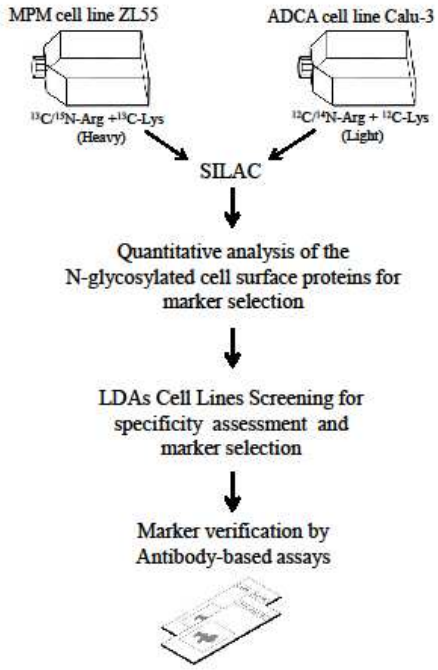

552 **Figure 1,** *Ziegler, Cerciello et al.*

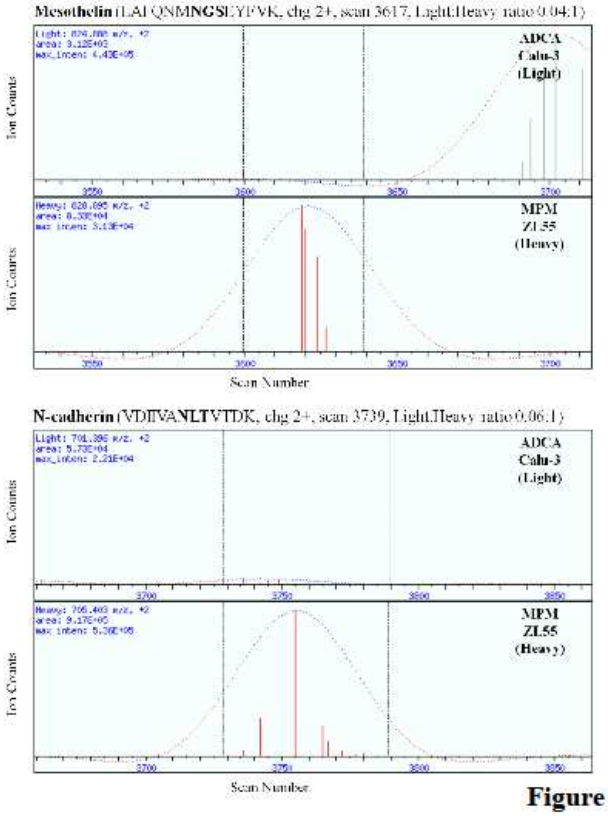

553 **Figure 2A,** *Ziegler, Cerciello et al.*

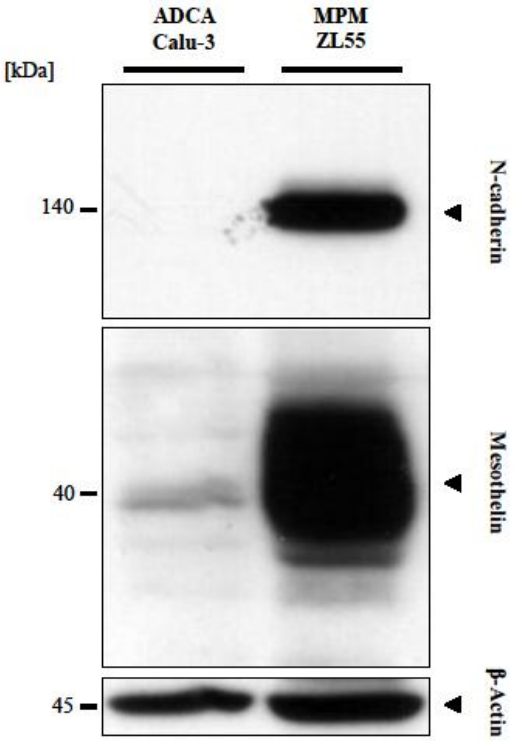

554 **Figure 2B,** *Ziegler, Cerciello et al.*

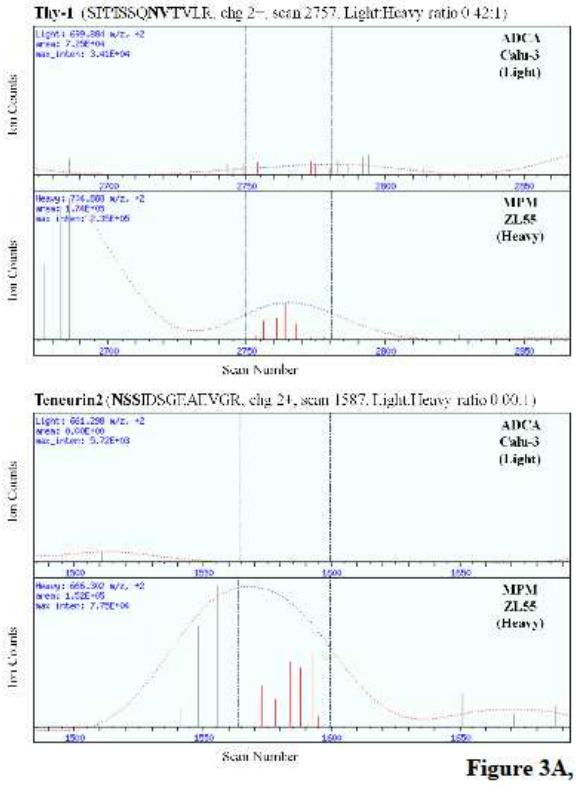

555 **Figure 3A,** *Ziegler, Cerciello et al.*

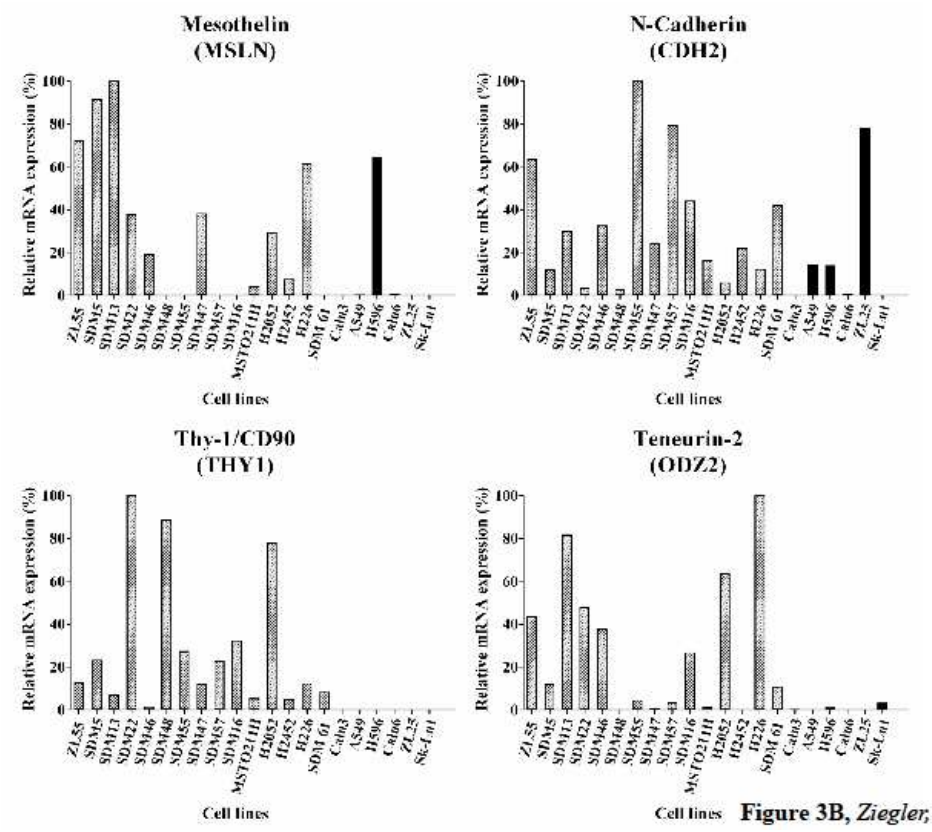

556 **Figure 3B,** *Ziegler, Cerciello et al.*

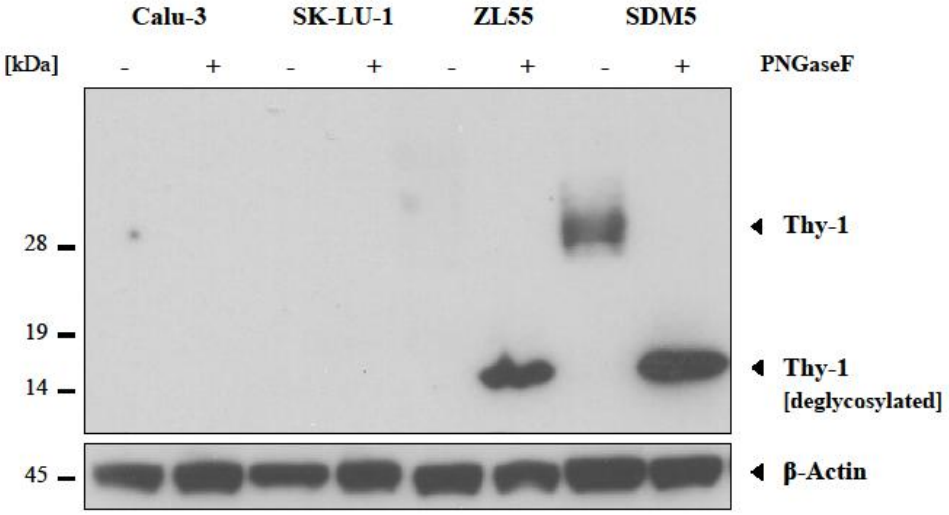

557 **Figure 4,** *Ziegler, Cerciello et al.*

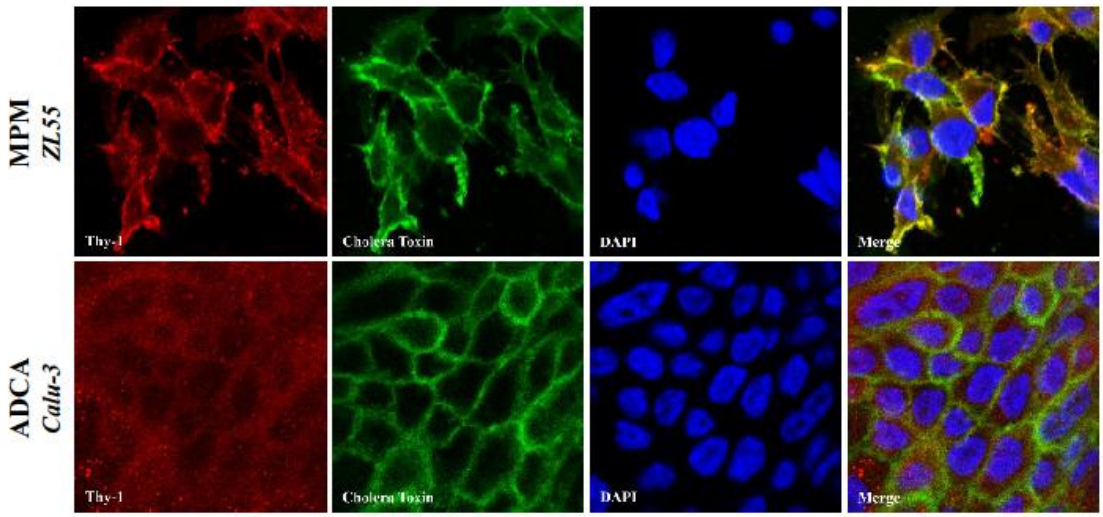

558 **Figure 5A,** *Ziegler, Cerciello et al.*

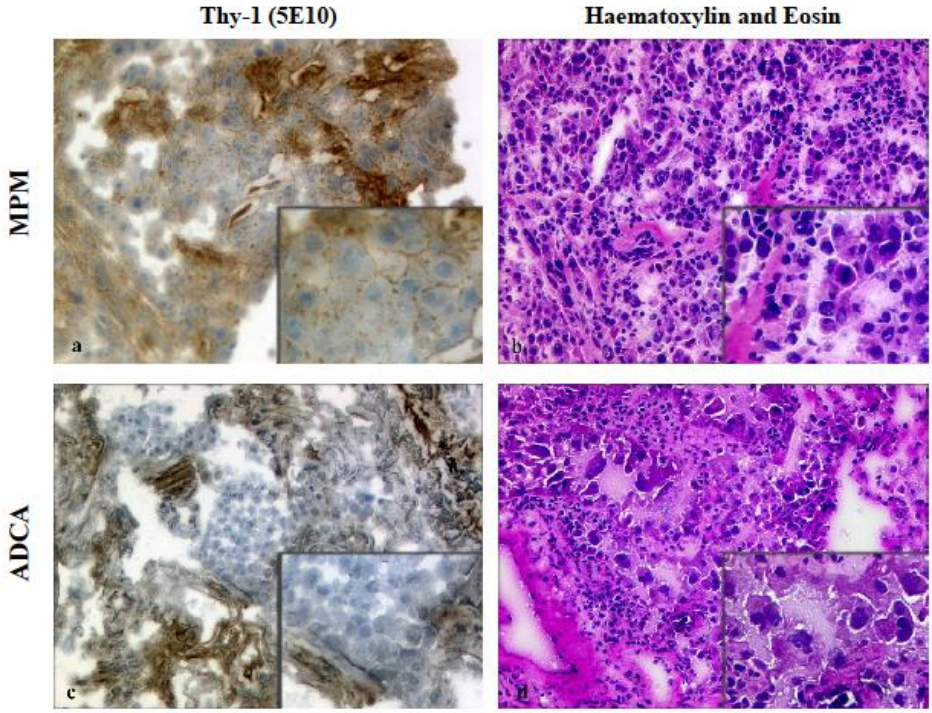

559 **Figure 5B,** *Ziegler, Cerciello et al.*